Inorg. Chem. **2003**, *42*, 2410–2417

Aggregation of PMe_3-Stabilized Molybdenum Sulfides and the Catalytic Dehydrogenation of H_2S

Daniel E. Schwarz, Thomas B. Rauchfuss,* and Scott R. Wilson

Department of Chemistry, University of Illinois, Urbana, Illinois 61801

Received November 26, 2002

The reactivity of $[MoS_4]^{2-}$ (**1**) toward PMe_3 was explored in the presence and absence of proton donors. Whereas MeCN solutions of $(Et_4N)_2[MoS_4]$ and PMe_3 are stable, in the presence of H_2S such solutions catalyze formation of H_2 and $SPMe_3$. Addition of NH_4^+ to such solutions afforded $MoS_2(PMe_3)_4$ (**2**), which can be prepared directly from $(NH_4)_2$[**1**]. Compound **2** is reactive toward thiols via a process proposed to involve the initial dissociation of one PMe_3 ligand, a hypothesis supported by the relative inertness of *trans*-$MoS_2(dmpe)_2$. Benzene solutions of **2** react with EtSH to give $Mo_2(\mu\text{-}S)(\mu\text{-}SH)(PMe_3)_4(SEt)_3$ (**3Et**). Analogous reactions with thiocresol (MeC_6H_4SH) and H_2S gave $Mo_2(\mu\text{-}S)(\mu\text{-}SH)(PMe_3)_4(SR)_3$ (R = tol, H). Crystallographic analyses of **3Et**, **3H**, and **3tol** indicate dinuclear species with seven terminal ligands and a $Mo_2(\mu\text{-}SR)(\mu\text{-}S)$ core (r_{Mo-Mo} = 2.748(1) Å). From reaction mixtures leading to **3Et** from **2**, we obtained the intermediate $Mo^{IV}_2(\mu\text{-}S)_2(SEt)_4(PMe_3)_2$ (**4**), an edge-shared bis(trigonal pyramidal) structure. Compounds **3H** and **3Et** react further with H_2S to give $Mo_4(\mu_2\text{-}S)_4(\mu_3\text{-}S)_2(PMe_3)_6(SH)_2$ (**5H**) and $Mo_4(\mu_2\text{-}S)_4(\mu_3\text{-}S)_2(PMe_3)_6(SEt)_2$ (**5Et**), respectively. Analogously, $W_4(\mu_2\text{-}S)_4(\mu_3\text{-}S)_2(PMe_3)_6(SH)_2$ was synthesized from a methanol solution of $(NH_4)_2WS_4$ with H_2S and PMe_3. A highly accurate crystallographic analysis of $(NH_4)_2MoS_4$ (R_1 = 0.0193) indicates several weak NH···S interactions.

Introduction

Molybdenum disulfide, MoS_2, is important in materials science and catalysis.[1−3] In recent years, Lewis base adducts of monomeric MoS_2 have been described, but the reactivity of these species remains largely unexplored.[4] In contrast, the behavior of cyclopentadienyl derivatives of molybdenum disulfide has been very fruitfully examined resulting in the discovery of several novel catalytic processes.[5] The species MoS_2L_4 (L = PR_3, SR_2), which are formal adducts of monomeric MoS_2,[6,7] are of interest because they could in principle oligomerize to afford polymetallic aggregates, which could exhibit new structural or catalytic properties.

A novel feature of MoS_2L_4 (L = 2e ligand) is the presence of the rarely observed "pure" M═S double bond; in most terminal sulfido complexes the M−S bond order is clearly above two.[8] The pure Mo═S functionality should exhibit distinctive behavior relative to derivatives where the MoS bonds order is >2. Thus, in this study our opening basic question focused on whether $MoS_2(PMe_3)_4$ is reactive at all or is simply a thermodynamic sink. We find that it is indeed reactive with regard to exchange of the phosphine ligands and reactions at the sulfido center. A second issue of interest was the possibility that $MoS_2(PMe_3)_4$ could serve as a monomer for the synthesis of larger Mo−S aggregates.

Prior work on the Mo_x−S−PR_3 system is presented in Scheme 1 for $1 \le x \le 4$ together with a summary of the preparative results in this paper and the numbering scheme used for the compounds. Aside from $MoS_2(PMe_3)_4$, other Mo−S−PR_3 species include tri-, tetra-, and hexametallic clusters, and dodecametallic clusters have been prepared primarily by Saito's group. These include $Mo_3S_5(PR_3)_6$,[9] $Mo_4S_6(SH)_2(PMe_3)_6$,[10] $Mo_6S_{10}(SH)_2(PEt_3)_6$,[10] and the Chevrel-like cluster $Mo_6S_8(PR_3)_6$ and its dimer $Mo_{12}S_{16}(PR_3)_{10}$.[11,12]

* To whom correspondence should be addressed. E-mail: rauchfuz@uiuc.edu.

(1) Daage, M.; Chianelli, R. R. *J. Catal.* **1994**, *149*, 414−427.
(2) Startsev, A. N. *Catal. Rev.—Sci. Eng.* **1995**, *37*, 353−423.
(3) Byskov, L. S.; Norskov, J. K.; Clausen, B. S.; Topsoe, H. *NATO ASI Ser., Ser. 3* **1998**, *60*, 155−168.
(4) Yoshida, T.; Adachi, T.; Matsumura, K.; Baba, K. *Angew. Chem.* **1993**, *105*, 1730−1732; *Angew. Chem., Int. Ed. Engl.* **1993**, *1732* (1711), 1621−1733.
(5) Rakowski DuBois, M. In *Catalysis by Di- and Polynuclear Metal Cluster Complexes*; Adams, R. D., Cotton, F. A., Eds.; Wiley-VCH: New York, 1998; pp 127−143.
(6) Cotton, F. A.; Schmid, G. *Inorg. Chem.* **1997**, *36*, 2267−2278.
(7) Parkin, G. *Prog. Inorg. Chem.* **1998**, *47*, 1−166.
(8) Coucouvanis, D. *Adv. Inorg. Chem.* **1998**, *45*, 1−73.
(9) Tsuge, K.; Imoto, H.; Saito, T. *Inorg. Chem.* **1995**, *34*, 3404−3409.

10.1021/ic026215m CCC: $25.00
Published on Web 03/07/2003

Scheme 1

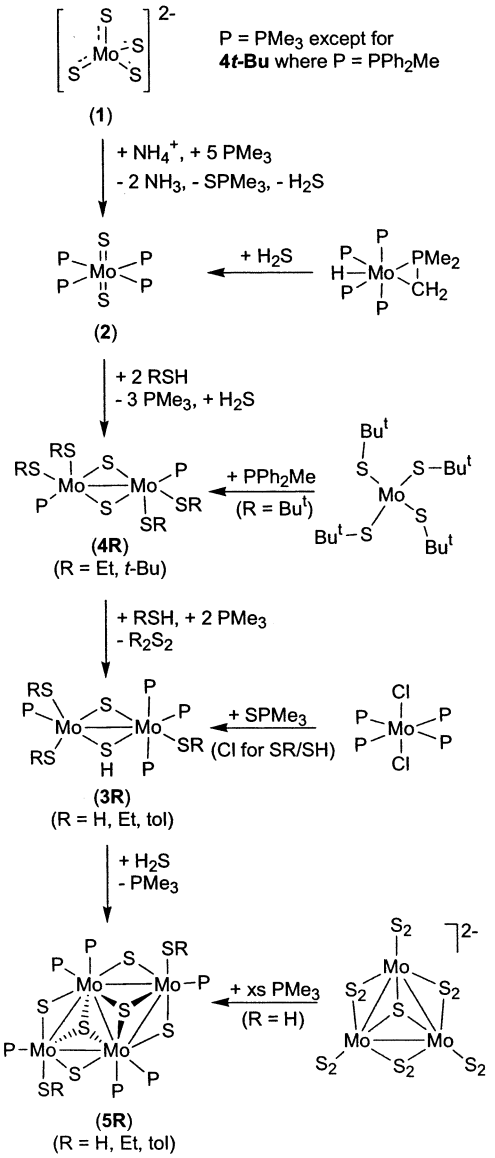

Results

Reactions of PMe$_3$ with [MoS$_4$]$^{2-}$. At the outset we sought to develop a new synthesis of $MoS_2(PMe_3)_4$, the prior one from "$Mo(PMe_3)_6$" requiring more specialized reagents.[13] To this end, we explored the reactivity of PMe_3 toward $[MoS_4]^{2-}$ (**1**) in the presence and absence of proton donors that could neutralize the negative charge on the thiometalate. Anhydrous MeCN solutions of $(Et_4N)_2[MoS_4]$ containing excess PMe_3 are stable at room temperature, as confirmed by UV−vis and ^{1}H NMR measurements. Addition of H_2S to such solutions results in the catalytic formation of H_2 and $SPMe_3$ (eq 1). Experiments were typically performed in sealed NMR tubes and analyzed by ^{1}H NMR spectroscopy. In the absence of **1**, benzene solutions of PMe_3 and H_2S are stable.

$$PMe_3 + H_2S \xrightarrow{(Et_4N)_2MoS_4} SPMe_3 + H_2 \qquad (1)$$

The concentration of **1** remains unaffected by the catalytic conversion. After 150 min at room temperature, 25.3 turnovers were observed. Solutions of $(Et_4N)_2$[**1**] also slowly catalyze the desulfurization of H_2S by PPh_3 to give $SPPh_3$ and H_2, with the addition of heat. At 65 °C, we observed approximately 25 turnovers in 72 h.

When MeCN solutions of $(Et_4N)_2$[**1**] were treated with both PMe_3 and NH_4^+, we obtained $MoS_2(PMe_3)_4$ (**2**). This transformation is more easily accomplished starting with $(NH_4)_2$[**1**], which is a routinely available salt.[14] The reaction is initially heterogeneous but is complete within 1 h to give the grass green product. A similar reaction of $(NH_4)_2[WS_4]$, H_2S, and PMe_3 in MeCN gave purple $WS_2(PMe_3)_4$.[15] Compound **2** and its W analogue were originally prepared by Parkin by the addition of H_2S to $M(PMe_3)_6$ (M = Mo, W).

Properties of MoS$_2$(PMe$_3$)$_4$. The reactivity of **2** toward H_2S and thiols, the primary focus of this report, is proposed to involve the initial dissociation of one PMe_3 ligand from **2**. Supporting this hypothesis, the ^{1}H NMR spectrum of a freshly prepared toluene solution of **2** exhibits a signal for free PMe_3 (δ 0.8) coincident with a color change from green to brown. The ratio of free to coordinated PMe_3 is 1:3. The brown solutions remain homogeneous for hours, although the ^{1}H and ^{31}P NMR spectra become increasingly complex indicative of cluster formation. An (−)ESI mass spectrum of the brown solution showed many signals. The most prominent at 906 *m*/*z* corresponds approximately to $Mo_4S_7(PMe_3)_4$; however, an exact fit was not achieved. At −90 °C, green solutions of **2** are stable, exhibiting a singlet at δ 1.5 corresponding to equivalent, coordinated PMe_3 ligands.

In contrast to the behavior of **2**, *trans*-$MoS_2(dmpe)_2$ (derived from treatment of **2** with two equiv dmpe) retains its green color in solution even at room temperature due to the chelating nature of the diphosphine (the corresponding dppe derivative is similar).[6] *trans*-$MoS_2(dmpe)_2$ does not react with organic thiols, in contrast to the behavior of **2** (see later).

Reaction of MoS$_2$(PMe$_3$)$_4$ with Thiols. Benzene solutions of **2** react with EtSH at room temperature over the course of hours to give $Mo_2(\mu\text{-}S)(\mu\text{-}SH)(PMe_3)_4(SEt)_3$ (**3Et**). The process can be rationalized according to eq 2.

$$\underset{\textbf{(2)}}{MoS_2(PMe_3)_4} + 3RSH \rightarrow \underset{\begin{array}{l}\textbf{(3H; R = H)}\\ \textbf{(3Et; R = Et)}\\ \textbf{(3tol; R = } p\text{-}MeC_6H_4\textbf{)}\end{array}}{Mo_2(S)(SH)(SR)_3(PMe_3)_4} + H_2S + SPMe_3 + 3PMe_3 \qquad (2)$$

The ^{1}H NMR spectrum of **3Et** displays separate signals for the four nonequivalent PMe_3 ligands. The mutually diaxial PMe_3 ligands are nonequivalent due to the pyramidal

(10) Tsuge, K.; Imoto, H.; Saito, T. *Inorg. Chem.* **1992**, *31*, 4715−4716.
(11) Saito, T. *Adv. Inorg. Chem.* **1997**, *44*, 45−91.
(12) Amari, S.; Imoto, H.; Saito, T. *Chem. Lett.* **1997**, 967−968.
(13) Murphy, V. J.; Parkin, G. *J. Am. Chem. Soc.* **1995**, *117*, 3522−3528.
(14) McDonald, J. W.; Friesen, G. D.; Rosenhein, L. D.; Newton, W. E. *Inorg. Chim. Acta* **1983**, *72*, 205−210.
(15) Rabinovich, D.; Parkin, G. *Inorg. Chem.* **1995**, *34*, 6341−6361.

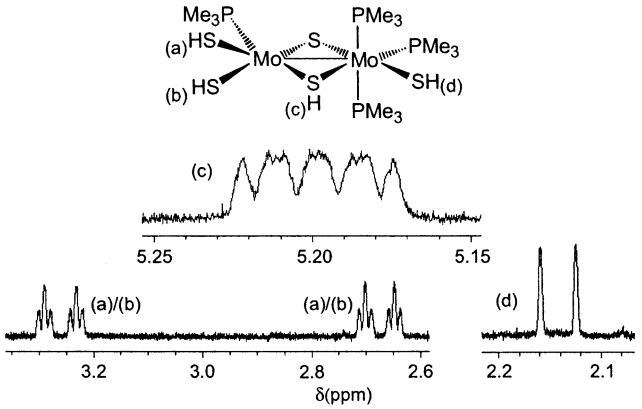

Figure 1. ^{1}H NMR (C_6D_6, 500 MHz, 298 K) spectrum of the S*H* signals for **3H** with assignments based on selectively decoupled ^{1}H{^{31}P} measurements. The assignments of H_a and H_b are ambiguous.

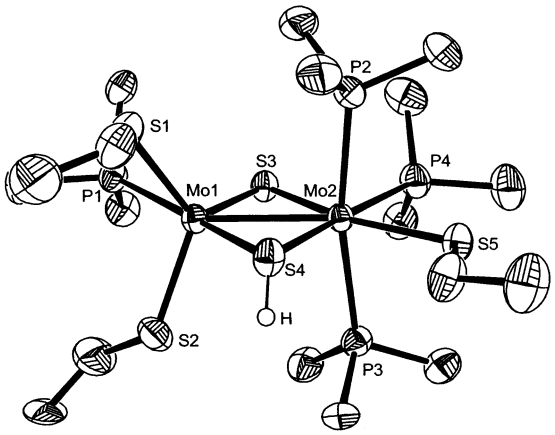

Figure 2. Molecular structure and atom numbering scheme of $Mo_2S(SH)(PMe_3)_4(SEt)_3$ (**3Et**).

nature of the μ-SH group, which lowers the symmetry of the complex to C_1. The S*H* signal appears as a complex multiplet at δ 5.20, which is downfield relative to the chemical shifts of related complexes with terminal MoSH ligands (vide infra). The ^{31}P NMR spectrum of **3Et** features three signals including an AB quartet for the diaxial phosphine ligands.

Reaction of **2** with thiocresol (p-MeC_6H_4SH) gave $Mo_2(\mu\text{-}S)(\mu\text{-}SH)(PMe_3)_4(Stol)_3$ (**3tol**), which is completely analogous to **3Et**, as indicated by NMR and X-ray crystallographic analyses.

Solutions of **2** react with H_2S in a manner analogous to the reaction involving organic thiols to give emerald green $Mo_2(\mu\text{-}S)(\mu\text{-}SH)(SH)_3(PMe_3)_4$ (**3H**). The efficiency of the reaction is greatly enhanced when performed in one pot by treatment of $(NH_4)_2$[**1**] with excess of both PMe_3 and H_2S. The role of the excess PMe_3 is not known, but purified samples of **2** react more slowly with H_2S than with organic thiols. Compound **3H**, being an unusual example of a complex with several inequivalent SH ligands, exhibits a structurally informative ^{1}H NMR spectrum (Figure 1). S*H* signals were assigned via a series of selective^{1}H{^{31}P} spectra. Only P−S*H* coupling was observed in the ^{1}H NMR spectrum. The PMe_3 signals were all doublets. The signals assigned to μ-SH in **3Et**, **3tol**, and **3H** were similar in terms of chemical shift and coupling pattern. ^{31}P NMR signals were assigned using ^{31}P−^{31}P correlation measurements (COSY).

Crystallographic analysis of **3Et** (Figure 2) reveals a dinuclear species with seven terminal ligands and two bridging sulfur atoms. The idealized coordination geometry at Mo(1) is trigonal bipyramidal, with P(1) and S(4) occupying the axial positions, $\angle$P(1)−Mo(1)−S(4) = 171.04(5)°. The trigonal plane is defined by S(1), S(2), and S(3), with $\sum\angle$S−Mo−S = 257°. The coordination geometry at Mo(2) can be described as distorted octahedral. With an $P(2)_{ax}$−Mo(2)−$P(3)_{ax}$ of 166.79(5)°, the axial phosphine ligands are bent away from the crowded binuclear core. Overall, **3Et** is an unusual example of an octahedron and a trigonal bipyramid fused along a common edge. Usually M_2L_9 dimers rearrange to form confacial bioctahedral structures with three bridging ligands, as seen in the similar species $Mo_2Cl_6(C_4H_8S)_3$.[16] The Mo−Mo distance is 2.748(1) Å. The central Mo_2S_2 core is planar, with the sum of the bond angles being 360°. The Mo−μ-S distances are 2.250(1) and 2.295(1) Å, much shorter than the corresponding Mo−(μ-SH) distances of 2.418(1) and 2.428(1) Å. The S*H*, which was located crystallographically, is pyramidal with the sum of the $\sum(\angle$Mo−S−X) = 285° (X = Mo, H). The structure of **3Et** is analogous to that of $Mo_2(\mu\text{-}S)(\mu\text{-}Cl)(PMe_3)_4Cl_3$.[17−19]

The structures of **3H** and **3tol** (not shown) are analogous to **3Et**. The protons of the four S*H* groups in **3H** were identified crystallographically. The M−M distance of 2.7081(6) Å for **3H** is slightly shorter than the one measured in **3Et**, probably as a consequence of the smaller size of SH versus SEt.

$Mo_2(\mu\text{-}S)_2(SR)_4(PMe_3)_2$, an Intermediate in the Formation of $Mo_2(\mu\text{-}S)(\mu\text{-}SH)(PMe_3)_4(SR)_3$ from $MoS_2(PMe_3)_4$. From some reaction mixtures affording **3Et** from **2**, we detected the intermediate $Mo_2(\mu\text{-}S)_2(SEt)_4(PMe_3)_2$ (**4Et**). We did not observe **4tol** or **4H** in the syntheses of **3tol** and **3H.** A small amount of **4Et** was crystallized and characterized by ^{1}H and ^{31}P NMR spectroscopy as well as by X-ray crystallography (Figure 3). The crystallographic study confirmed the edge-shared bis(trigonal pyramidal) structure analogous to that previously observed in $Mo_2(\mu\text{-}S)_2(SBu\text{-}t)_4(PMePh_2)_2$.[20] The C$H_2$ signals in the ^{1}H NMR spectrum are nonequivalent, indicating that the complex is stereochemically rigid.

On a preparative scale, treatment of **4Et** with further equivalents of EtSH and PMe_3 gave **3Et**, consistent with the fact that this $[Mo(IV)]_2$ species is an intermediate in the conversion of **2** into **3Et** (eq 3).

In principle, this reaction should produce Et_2S_2, but attempts to monitor this reaction by sealed-tube NMR experiments were not successful.

(16) Moynihan, K. J.; Gao, X.; Boorman, P. M.; Fait, J. F.; Freeman, G. K. W.; Thornton, P.; Ironmonger, D. J. *Inorg. Chem.* **1990**, *29*, 1648−1654.
(17) Hall, K. A.; Mayer, J. M. *Inorg. Chem.* **1995**, *34*, 1145−1158.
(18) Hall, K. A.; Critchlow, S. C.; Mayer, J. M. *Inorg. Chem.* **1991**, *30*, 3593−3594.
(19) Hall, K. A.; Mayer, J. M. *Inorg. Chem.* **1994**, *33*, 3289−3298.
(20) Kamata, M.; Yoshida, T.; Otsuka, S.; Hirotsu, K.; Higushi, T. *J. Am. Chem. Soc.* **1981**, *103*, 3572−3574.

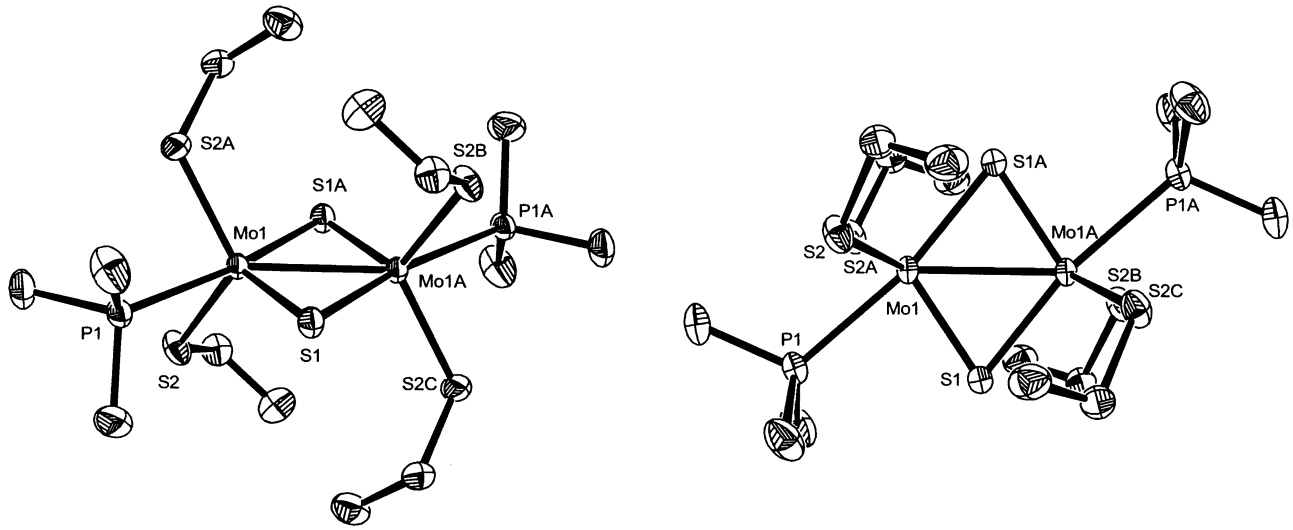

Figure 3. Two views showing the molecular structure and atom numbering scheme of $Mo_2S_2(SEt)_4(PMe_3)_2$ (**4Et**). Selected distances (Å) and angles (deg): Mo(1)−S(1) 2.2461(7), Mo(1)−S(2) 2.3255(7), Mo(1)−P(1) 2.5573(8), Mo(1)−Mo(1A) 2.7152(9), S(1)−Mo(1)−S(2) 117.49(1), S(1)−Mo(1)−S(2A) 117.49(1), S(2)−Mo(1)−S(2A) 117.12(3), S(1)−Mo(1)−P(1) 82.28(3), S(1A)−Mo(1)−P(1) 169.83(1).

$$Mo_2(S)_2(SEt)_4(PMe_3)_2 + EtSH + 2\ PMe_3 \rightarrow \underset{\textbf{(4Et)}}{} \qquad Mo_2(S)(SH)(SEt)_3(PMe_3)_4 + Et_2S_2 \quad (3)$$
$$\textbf{(3Et)}$$

Reactions of $Mo_2(\mu$-S)(μ-SH)$(PMe_3)_4(SR)_3$ with H_2S. Compounds **3H** and **3Et** were found to react further with H_2S to give tetranuclear products $Mo_4(\mu_2\text{-}S)_4(\mu_3\text{-}S)_2(PMe_3)_6(SH)_2$ (**5H**) and $Mo_4(\mu_2\text{-}S)_4(\mu_3\text{-}S)_2(PMe_3)_6(SEt)_2$ (**5Et**) (Figure 4), respectively. These species were characterized by ^{1}H and ^{31}P NMR spectroscopy and X-ray crystallography. ^{1}H NMR spectroscopic characterization of the conversion of **3H** into **5H** revealed the formation of H_2, PMe_3, and $SPMe_3$. Compound **5H** also catalyzes the conversion of H_2S and PMe_3 to $SPMe_3$ and H_2, although at a much slower rate than does $(Et_4N)_2$[**1**]. Spectroscopically, the conversion of **3H** into **5H** is quantitative; the isolation of **5H** is facilitated because of its low solubility. Saito had previously prepared compound **5H** via the reaction of butylamine−THF solutions of $(NH_4)_2[Mo_3S(S_2)_6]$ and PMe_3, although spectroscopic characterization was not reported.[21] Compounds **5H** and **5Et** also form when solutions of **2** containing RSH are allowed to stand. Compound **5tol** was not detected.

$W_4(\mu_2\text{-}S)_4(\mu_3\text{-}S)_2(PMe_3)_6(SH)_2$, which is structurally analogous to **5H**, was synthesized from a methanol solution of $(NH_4)_2WS_4$ with excess H_2S and PMe_3. The ^{1}H and ^{31}P NMR signals match those observed in **5H**. A derivative of this species, $W_4(\mu_2\text{-}S)_4(\mu_3\text{-}S)_2(PMe_2Ph)_6(SH)_2$, had been previously synthesized via treatment of $W(N_2)_2(PMe_2Ph)_4$ with $(Me_3Si)_2S$ and MeOH,[22] conditions conducive to in situ formation of H_2S. Previous workers did not detect the S*H* signals in the ^{1}H NMR spectrum for $W_4(\mu_2\text{-}S)_4(\mu_3\text{-}S)_2(PMe_2Ph)_6(SH)_2$.

The structures of **5H** and **5Et** were confirmed crystallographically. The four molybdenum atoms of the tetrametallic cluster define a parallelogram, the cluster symmetry being approximately C_{2h}. Each of two Mo_3 triangles is capped with μ_3-S ligands on opposite sides of the Mo_4 plane. Each exterior Mo−Mo bond is spanned by a μ_2-S while the two "hinge" Mo atoms have PMe_3 ligands, and the "wing-tip" Mo atoms feature both PMe_3 and terminal SR ligands.

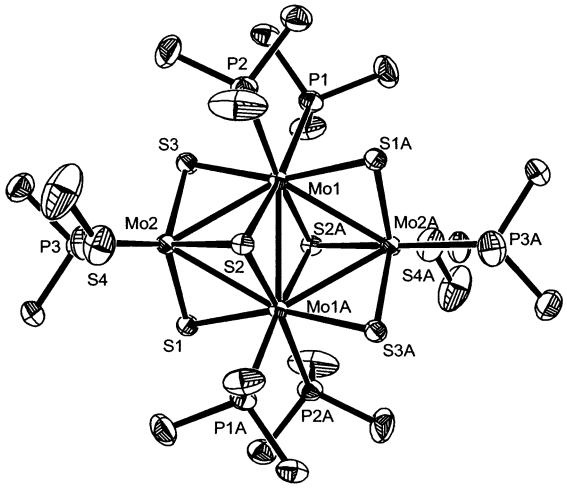

Figure 4. Molecular structure and atom numbering scheme of $Mo_4S_6(SEt)_2(PMe_3)_6$ (**5Et**). Selected distances (Å) and angles (deg): Mo(1)−Mo(2) 2.8345(9), Mo(1)−Mo(1A) 2.841(1), Mo(2)−S(4) 2.393(1), Mo(1)−Mo(2)−Mo(1A) 60.14(1), Mo(2)−Mo(1)−Mo(2A) 119.85(1).

Crystallographic Reexamination of $(NH_4)_2MoS_4$. Because NH_4^+ significantly influences the chemical behavior of MoS_4^{2-}, we sought some insights into the hydrogen bonding in crystalline $(NH_4)_2MoS_4$, which was characterized at lower resolution that did not reveal hydrogen atom positions.[23] A particularly high quality refinement (R_1 = 0.0193) allowed us to locate the hydrogen atoms, which are disordered over two orientations of both NH_4^+ cations.

(21) Tsuge, K.; Mita, S.; Fujita, H.; Imoto, H.; Saito, T. *J. Cluster Sci.* **1996**, *7*, 407−421.

(22) Kuwata, S.; Mizobe, Y.; Hidai, M. *J. Chem. Soc., Dalton Trans.* **1997**, 1753−1758.

(23) Lapasset, J.; Chezeau, N.; Belougne, P. *Acta Crystallogr., Sect. B* **1976**, *B32*, 3087−3088.

The N···S distances for one of the cations fall in the range 3.26−3.53 Å, typical, if slightly long, for a hydrogen bond to sulfur.[24,25] The N···S distances for the second cation are longer, in the range 3.50−3.62 Å. The H···S distances range from 2.55 to 3.02 Å. The Mo−S bonds are within 0.01 Å of those for in $[Et_4N]_2MoS_4$.[26]

Discussion

The goal of this research was to extend our recently reported reaction of PMe_3, H_2S, and ReS_4^-, which gives the catalytically active species $ReH(SH)_2(PMe_3)_4$.[27] Extension of the $PMe_3 + H_2S$ reaction to $(NH_4)_2[MS_4]$ (M = Mo, W) led to efficient syntheses of $MoS_2(PMe_3)_4$ and $WS_2(PMe_3)_4$. Furthermore, the reactivity of the resulting $MoS_2(PMe_3)_4$ revealed previously unnoticed relationships between various Mo−S−PR_3 compounds (Scheme 1). $MoS_2(PMe_3)_4$ (as well as $WS_2(PMe_3)_4$) was originally prepared by Parkin via an elegant but somewhat arduous route involving the addition of H_2S to $Mo(PMe_3)_6$.[13] It was proposed that this conversion proceeded via the intermediacy of the metastable $MoH_2(SH)_2(PMe_3)_4$,[15] which is analogous to the robust species $ReH(SH)_2(PMe_3)_4$.[27]

A significant finding is that the reactivity of $[MoS_4]^{2-}$ is sensitive to the presence of protic reagents. The nonreactivity of PMe_3 toward $(Et_4N)_2[MoS_4]$ is attributed to the high charge/atom for hypothetical desulfurized product $\{[MoS_3]^{2-}\}_n$. Despite its apparent nonreactivity toward PMe_3, $(Et_4N)_2[MoS_4]$ catalyzes the reaction of PMe_3 and H_2S to give $SPMe_3$ and H_2. Hoff et al. have determined the enthalpy of the reaction $PMe_3 + {}^1/_8S_8 \rightarrow SPMe_3$ to be −27.1 kcal/mol.[28] The heat of formation of H_2S is −4.93 kcal/mol.[29] The enthalpy of the new dehydrogenation reaction is thus calculated to be −22.17 kcal/mol (Scheme 2). Hoff et al. also reported the enthalpy of reaction for $PPh_3 + {}^1/_8S_8$ to form $SPPh_3$ to be −21.5 kcal/mol which corresponds to −16.57 kcal/mol for the analogous dehydrogenation of H_2S by PPh_3.

Scheme 2

$PMe_3 + {}^1/_8S_8 \rightarrow SPMe_3$	ΔH = -27.1	kcal/mol
$H_2S \rightarrow H_2 + {}^1/_8S_8$	4.93	kcal/mol
$PMe_3 + H_2S \rightarrow SPMe_3 + H_2$	-22.17	kcal/mol

In view of the nonreactivity of PMe_3 toward $(Et_4N)_2[MoS_4]$, it is logical that that the catalytic process is initiated by a reaction of H_2S with $[MoS_4]^{2-}$. Such H_2S-initiated reactions could afford $[MoS_3(SH)]^-$, resulting from protonation by H_2S, or $[MoS_3(SH)_2]^{2-}$, resulting from the addition of H_2S across a Mo═S bond. H_2 formation may indicate a

Scheme 3

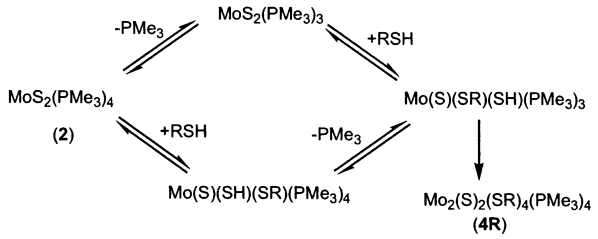

Mo−H species that undergoes protonation by H_2S or intramolecularly by a MoSH group, but insufficient information is available to allow us to formulate a mechanism. Protonation of $[MoS_4]^{2-}$ is reasonable in view of the existence of $WS_2(SH)_2$[30] and $[EtSMoS_3]^-$.[31] Nucleophilic attack of tertiary phosphine ligands at electrophilic nitrido ligands[32,33] provides a suitable precedent for the reaction Mo^{VI}═S + PMe_3. Also potentially relevant is the recent report of phosphine adducts of d^0-tungsten sulfides, e.g., $[WS_3(SR)(PR_3)]^-$.[34] Several reports describe the $Pd_2X_2(dppm)_2$-catalyzed conversion of $H_2S + CH_2(PPh_2)_2 \rightarrow H_2 + CH_2(PPh_2)(P(S)Ph_2)$.[35−37] These reactions occur at room temperature with 20 turnovers over a few hours.

The nonreactivity of PMe_3 toward $(Et_4N)_2[MoS_4]$ contrasts with the efficient desulfurization of $(NH_4)_2[MoS_4]$ to give $MoS_2(PMe_3)_4$. NH_4^+ (pK_a (MeCN) = 16.5)[38] facilitates the loss of SH^- from $[MoS_4]^{2-}$, allowing the formation of the neutral derivatives. Ammonium salts of $[Mo_3S_{13}]^{2-}$ undergo phosphine-induced cluster building reactions; in such a case, the NH_4^+ likely also facilitates the desulfurization.[9,10] A detailed crystallographic analysis of $(NH_4)_2MoS_4$ does not reveal any striking H···S distances, perhaps because the large number of such interactions precludes a single strong interaction.

The reaction of **2** with RSH reagents gives the molybdenum(IV) species, $Mo_2S_2(SR)_4(PMe_3)_2$, as the first isolable adduct. Two plausible pathways for this conversion are presented in Scheme 3; they differ with respect to the timing of dissociation of PMe_3, but in each case, the key reaction is the addition of RSH across a Mo═S bond.

The addition of RSH across M═S has been observed for the d^2 derivatives $[ReS_2(S_2C_2R_4)]^-$.[39] For example, $[ReS_2(S_2C_2H_4)]^-$ adds PhSH to give square pyramidal $[ReS(SPh)(SH)(S_2C_2H_4)]^-$.[39] In non-$d^0$ systems, S-to-metal π-donation is less important than in d^0 analogues. In such cases, S═M

(24) Krepps, M. K.; Parkin, S.; Atwood, D. A. *Cryst. Growth Des.* **2001**, *1*, 291−297.
(25) McGuire, D. G.; Khan, M. A.; Ashby, M. T. *Inorg. Chem.* **2002**, *41*, 2202−2208.
(26) Kanatzidis, M. G.; Coucouvanis, D. *Acta Crystallogr., Sect. C: Cryst. Struct. Commun.* **1983**, *C39*, 835−838.
(27) Schwarz, D. E.; Dopke, J. A.; Rauchfuss, T. B.; Wilson, S. R. *Angew. Chem., Int. Ed.* **2001**, *40*, 2351−2353.
(28) Capps, K. B.; Wixmerten, B.; Bauer, A.; Hoff, C. D. *Inorg. Chem.* **1998**, *37*, 2861−2864.
(29) Weast, R. C. CRC Press: Boca Raton, FL, 1987.
(30) Gattow, G.; Franke, A. *Z. Anorg. Allg. Chem.* **1967**, *352*, 246−251.
(31) Kruhlak, N. L.; Wang, M.; Boorman, P. M.; Parvez, M. *Inorg. Chem.* **2001**, *40*, 3141−3148.
(32) Huynh, M. H. V.; Jameson, D. L.; Meyer, T. J. *Inorg. Chem.* **2001**, *40*, 5062−5063.
(33) Crevier, T. J.; Bennett, B. K.; Soper, J. D.; Bowman, J. A.; Dehestani, A.; Hrovat, D. A.; Lovell, S.; Kaminsky, W.; Mayer, J. M. *J. Am. Chem. Soc.* **2001**, *123*, 1059−1071.
(34) Arikawa, Y.; Kawaguchi, H.; Kashiwabara, K.; Tatsumi, K. *Inorg. Chem.* **2002**, *41*, 513−520.
(35) Wong, T. Y. H.; Rettig, S. J.; James, B. R. *Inorg. Chem.* **1999**, *38*, 2143−2149.
(36) James, B. R. *Pure Appl. Chem.* **1997**, *69*, 2213−2220.
(37) Wong, T. Y. H.; Barnabas, A. F.; Sallin, D.; James, B. R. *Inorg. Chem.* **1995**, *34*, 2278−2286.
(38) Izutsu, K. *Acid−Base Dissociation Constants in Dipolar Aprotic Solvents*; Blackwell Scientific Publications: Oxford, 1990; Vol. 35.

Scheme 4. Schematic Description of the Condensation of **3H** to **5H**

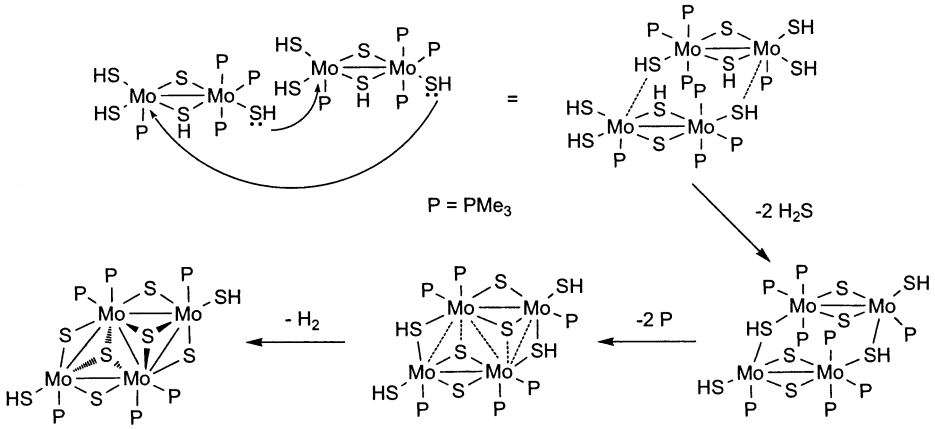

is more nearly equivalent to the $(RS)_2M$ in an energetic sense.[7] In contrast for d^0-Mo^{IV}, two thiolates are poor substitutes for the 3−4e S^{2-} common to d^0-Mo^{VI}, hence the nonreactivity of $[MoS_4]^{2-}$ toward thiols.

Compounds of the type $Mo_2E_2(ER)_4L_2$ (E = O, S, N; L = neutral donor ligand) were previously generated by Otsuka et al. via the decomposition of $Mo(S\text{-}t\text{-}Bu)_4$ in the presence of PPh_2Me.[20] In the Otsuka case, the sulfido ligands arise by fragmentation of the *tert*-butylthiolate ligands.[40] The species $Mo_2S_2(SEt)_4(PMe_3)_2$ (**4Et**) reacts with additional EtSH in a formal redox process to give the Mo(III) derivative $Mo_2(\mu\text{-}S)(\mu\text{-}SH)(SEt)_3(PMe_3)_4$ (**3Et**) which is related to $Mo_2(\mu\text{-}S)(\mu\text{-}Cl)Cl_3(PMe_3)_4$.[19] The similarity of these two compounds illustrates the occurrence of many SH analogues for early metal chlorides.[41,42]

Condensation of $Mo_2(\mu\text{-}S)(\mu\text{-}SR)(SR)_3(PMe_3)_4$ occurs at room temperature in the presence of H_2S or by allowing the reaction of **2** and H_2S to proceed to produce $Mo_4(\mu_2\text{-}S)_4(\mu_3\text{-}S)_2(SR)_2(PMe_3)_6$, a mixed valence $[Mo(III)]_2[Mo(IV)]_2$ species. This partial reoxidation is proposed to proceed via loss of H_2 (eqs 4−5).

$$4H_2S + 2Mo_2(S)(SR)(SR)_3(PMe_3)_4 \rightarrow Mo_4S_6(SR)_2(PMe_3)_6 + 4RSH + H_2 + 2PMe_3 \quad (4)$$

$$2Mo_2(S)(SH)_4(PMe_3)_4 \rightarrow Mo_4S_6(SR)_2(PMe_3)_6 + 2H_2S + H_2 + 2PMe_3 \quad (5)$$

A cartoon for the $2Mo_2 \rightarrow Mo_4$ assembly process is presented in Scheme 4. Saito has extended the Mo−S−SR−PR_3 series to $Mo_6S_{10}(SH)_2(PEt_3)_6$, where the formal Mo oxidation states are $[Mo(III)]_2[Mo(IV)]_4$ and the Mo/S ratio remains 1:2 as in MoS_2.[10] But we do not observe such further condensations.

Experimental Section

The salts $(NEt_4)_2MoS_4$, $(NEt_4)_2WS_4$, $(NH_4)_2WS_4$, and $(NH_4)_2MoS_4$ were synthesized by previously reported methods.[14] Spectroscopic methods have been described previously.[27] Most reactions were conducted on a vacuum line, which facilitated the transfer of the volatile reagents, and worked up using Schlenk techniques. Solutions of compounds **2**−**5** decompose under prolonged vacuum with formation of $SPMe_3$.

$MoS_2(PMe_3)_4$ (2).[13] Onto a frozen slurry of 300 mg (1.15 mmol) of $(NH_4)_2MoS_4$ in 10 mL of MeCN was condensed 0.7 mL (6.8 mmol) of PMe_3. The vessel was evacuated, sealed, and then allowed to warm to room temperature. The solution was stirred for 2 h during which the solution became green and a green precipitate formed. The solvent was then removed via filter cannula leaving an emerald green powder. The solid was then quickly dried in vacuo. X-ray quality crystals were grown from the mother liquor at −20 °C. Yield: 490 mg (89%). Anal. Calcd for $C_{12}H_{36}MoP_4S_2$ (Found): C, 31.04 (30.93); H, 7.81 (7.99); P, 26.68 (26.39); Mo, 20.66 (22.52). ^{1}H NMR (C_6D_6, 500 MHz, 298 K): δ 1.52 (br s).

$(NEt_4)_2MoS_4$-Catalyzed Reaction of H_2S and PMe_3. A sealed NMR tube containing 0.8 mg of $(Et_4N)_2MoS_4$, approximately 50× excess of PMe_3, approximately 20× excess of H_2S, and 0.8 mL of CD_3CN was monitored by ^{1}H NMR spectroscopy for 3 h at room temperature after initial thawing. Measurements were taken every 30 min. The quantity of $SPMe_3$ (d, δ 1.7) produced was integrated versus the methylene signal of Et_4N^+ (q, δ 3.2).

$WS_2(PMe_3)_4$. Onto a frozen slurry of 101 mg (0.29 mmol) of $(NH_4)_2WS_4$ in 20 mL of MeOH was condensed 0.7 mL (6.8 mmol) of PMe_3 and 310 mg (9.1 mmol) of H_2S. The vessel was evacuated, sealed, and then allowed to warm to room temperature. The solution was stirred for 5 h during which the solution became purple. Approximately 10 mL of the solvent was removed in vacuo, and a purple microcrystalline solid formed. The remaining solvent was removed via cannula, and the solid was dried in vacuo. The ^{1}H NMR data matches what was previously reported.[15] Yield: 140 mg (87%). ^{1}H NMR (C_6D_6, 500 MHz, 298 K): δ 1.67 (m). ^{31}P NMR (C_6D_6, 298 K): δ −44.1 (t).

$Mo_2S(SH)(PMe_3)_4(SEt)_3$ (3Et). A solution of 0.2 mL (2.7 mmol) of EtSH in 20 mL of MeCN was added to 131 mg (0.282 mmol) of **2** via cannula. The solution was stirred for 2 h with a slow N_2 purge and then filtered and stored overnight at −20 °C to give small green needles. Yield: 42 mg (20%). X-ray quality crystals were grown from saturated MeCN solutions of **3Et** at −20 °C. This solid was slightly contaminated with the $SPMe_3$ byproduct. ^{1}H NMR (C_6D_6, 500 MHz, 298 K): δ 5.20 (m, 1H), 4.11 (m, 1H), 3.97 (m, 1H), 3.70 (m, 1H), 3.17−3.00 (signals overlap, m, 3H), 2.16 (d, 9H), 1.88 (t, 3H), 1.68 (d, 9H), 1.50 (t, 3H), 1.40 (t, 3H), 0.61 (d, 9H), 0.49 (d, 9H). ^{31}P NMR (C_6D_6, 298 K): δ 7.04 (td, 1P), −3.48 (td, 1P), −13.15 (AB quartet, 2P).

$Mo_2S(SH)_4(PMe_3)_4$ (3H). On to a frozen slurry of 200 mg (0.77 mmol) of $(NH_4)_2MoS_4$ in 20 mL of MeCN was condensed 0.7 mL

(39) Dopke, J. A.; Rauchfuss, T. B.; Wilson, S. R. *Inorg. Chem.* **2000**, *39*, 5014−5021.
(40) Coucouvanis, D.; Hadjikyriacou, A.; Lester, R.; Kanatzidis, M. G. *Inorg. Chem.* **1994**, *33*, 3645−3655.
(41) Peruzzini, M.; De Los Rios, I.; Romerosa, A. *Prog. Inorg. Chem.* **2001**, *49*, 169−453.
(42) Kuwata, S.; Hidai, M. *Coord. Chem. Rev.* **2001**, *213*, 211−305.

Table 1. Details of Data Collection and Structure Refinement for **3H**, **3Et**, **3tol**, **4Et**, **5H**, and **5Et**

	3H	3Et	3tol	4Et	5H	5Et
formula·solvate	C12H46Mo2N2P4S5·2CH$_3$CN	C18H52Mo2P4S5·0.5CH$_3$CN	C33H58Mo2P4S5·0.5Et$_2$O	C14H38Mo2P2S6	C25H64Mo4P6S8	C22H64Mo4P6S8
cryst size (mm^3)	0.60 × 0.06 × 0.06	0.40 × 0.04 × 0.03	0.30 × 0.14 × 0.02	0.35 × 0.26 × 0.20	0.13 × 0.04 × 0.015	0.22 × 0.13 × 0.12
space group	$P\bar{3}$	$C2/c$	$P2_1/c$	$Cmca$	$P\bar{1}$	$P2_1/n$
a (Å)	23.805(2)	43.165(16)	10.105(5)	13.490(4)	9.887(5)	11.605(4)
b (Å)	23.805(2)	9.645(4)	22.454(11)	16.068(5)	11.314(6)	10.482(4)
c (Å)	10.3094(15)	17.008(6)	20.593(10)	12.599(4)	11.405(6)	19.856(7)
α (deg)	90	90	90	90	69.042(9)	90
β (deg)	90	100.198(7)	101.225(10)	90	84.116(10)	104.113(6)
γ (deg)	120	90	90	90	79.885(10)	90
V (Å^3)	5059.2(10)	6969(5)	4583(4)	2731.1(15)	1171.9(11)	2342.5(15)
Z	6	8	4	4	1	2
D_{calcd} (Mg m^{-3})	1.462	1.459	1.403	1.587	1.687	1.637
μ (Mo Kα, mm^{-1})	1.251	1.212	0.939	1.493	1.625	1.623
max/min trans	0.9436/0.6473	0.9667/0.7542	0.9804/0.8292	0.7436/0.6345	0.9778/0.8819	0.8604/0.7260
reflns measd/indep	39717/6213	20461/6170	28268/8474	10321/1742	8893/4124	15326/4281
restraints/params	7/295	49/325	148/504	0/101	57/223	0/191
GOF	0.93	0.879	0.883	1.105	0.945	1.026
R_{int}	0.104	0.0946	0.2488	0.0355	0.0782	0.0459
R1 [$I > 2\sigma$] (all data)[a]	0.0353(0.0701)	0.0420(0.1115)	0.0729(0.2324)	0.0154(0.0170)	0.0530(0.1036)	0.0276(0.0448)
wR2 [$I > 2\sigma$] (all data)[b]	0.0578(0.0642)	0.0574(0.0681)	0.1109(0.1484)	0.0388(0.0394)	0.1241(0.1558)	0.0588(0.0626)
max peak/hole (e$^-$/Å^3)	0.453/ −0.454	0.604/−0.443	1.138/−0.768	0.470/−0.273	1.422/−1.477	0.732/−0.390

[a] $R1 = \sum||F_o| - |F_c||/\sum|F_o|$. [b] $wR2 = \{\sum[w(F_o^2 - F_c^2)^2]/\sum[w(F_o^2)^2]\}^{1/2}$.

(6.8 mmol) of PMe_3 and 310 mg (9.1 mmol) of H_2S. The vessel was evacuated, sealed, and then allowed to warm to room temperature. The mixture was stirred for 2 h during which it became homogeneous and turned green. The solvent volume was reduced to half in vacuo, and the remaining solvent was removed via cannula, leaving a green microcrystalline product. Yield: 270 mg (53%). This solid was slightly contaminated with the $SPMe_3$ byproduct. The yield was estimated by ^{1}H NMR determination of the **3H**/$SPMe_3$ ratio. X-ray quality crystals were grown from an MeCN solution at −20 °C. Further large needles were grown by vapor diffusion of Et_2O into MeCN, and these crystals were used for elemental analysis. Anal. Calcd for $C_{12}H_{40}Mo_2P_4S_5$·0.5 Et_2O (Found): C, 24.32 (24.10); H, 6.54 (6.50); P, 17.67 (17.76); Mo, 27.36 (27.51). ^{1}H NMR (C_6D_6, 500 MHz, 298 K): δ 5.21 (m, 1H), 3.27 (dt, 1H), 2.68 (dt, 1H), 2.15 (d, 1H), 1.97 (d, 9H), 1.56 (d, 9H), 0.64 (d, 9H), 0.46 (d, 9H). ^{31}P NMR (C_6D_6, 298 K): δ 11.65 (td, 1P), −1.32 (td, 1P), −14.89 (AB quartet, 2P). Crystals of **3H** slowly decompose to **5H** in the solid state, even in a nitrogen-purged glovebox.

$Mo_2S(SH)(PMe_3)_4(SC_6H_4Me)_3$ (3tol). To 205 mg (0.431 mmol) of **2** was transferred a solution of 65 mg (1.6 mmol) of 4-MeC_6H_4SH in 20 mL of MeCN. The slurry was stirred for 2 h with a slow N_2 purge and then filtered and stored at −20 °C overnight. Small crystals were collected by removal of the solvent via cannula. Yield: 79 mg (19%). ^{1}H NMR (C_6D_6, 500 MHz, 298 K): δ 8.22 (d, 2H), 7.73 (dd, 4H), 6.93 (m, 6H), 5.35 (m, 1H), 2.06 (s, 3H), 2.05 (s, 3H), 2.04 (s, 3H), 2.02 (d, 9H), 1.76 (d, 9H), 0.51 (d, 9H), 0.40 (d, 9H). ^{31}P NMR (C_6D_6, 298 K): δ 4.15 (td, 1P), −6.20 (td, 1P), −13.59 (AB quartet, 2P).

$Mo_2S_2(SEt)_4(PMe_3)_2$ (4Et). Onto 100 mg (0.215 mmol) of **2** was transferred a solution of 0.4 mL (5.4 mmol) of EtSH in 20 mL of MeCN. The solution was stirred for 1 h with a brisk N_2 purge and then stored at −20 °C. Small dark green crystals grew over 24 h and were collected by removal of the solvent via cannula. ^{1}H NMR (C_6D_6, 500 MHz, 298 K): δ 3.06 (dq, 4H), 2.85 (dq, 4H), 2.20 (m, 18H), 0.90 (t, 12H). ^{31}P NMR (C_6D_6, 298 K): δ 0.457 (s, 2P). These samples were invariably contaminated with **3Et**; further attempts at purification were unsuccessful. Addition of >10 equiv of EtSH and PMe_3 to MeCN solutions of **4Et** produce **3Et**, as observed by a sealed tube NMR experiment.

Table 2. Selected Bond Lengths (Å) and Angles (deg) for $Mo_2S(SH)(PMe_3)_4(SEt)_3$ (**3Et**)

Mo(1)−S(1)	2.357(1)	Mo(2)−S(5)	2.475(1)
Mo(1)−S(2)	2.307(1)	Mo(1)−P(1)	2.501(1)
Mo(1)−S(3)	2.250(1)	Mo(2)−P(2)	2.525(1)
Mo(1)−S(4)	2.418(1)	Mo(2)−P(3)	2.535(1)
Mo(2)−S(3)	2.295(1)	Mo(2)−P(4)	2.512(1)
Mo(2)−S(4)	2.428(1)	Mo(1)−Mo(2)	2.748(1)
Mo(1)−S(3)−Mo(2)	74.40(5)	S(1)−Mo(1)−S(2)	117.44(5)
Mo(1)−S(4)−Mo(2)	69.08(4)	S(2)−Mo(1)−S(3)	118.61(6)
S(4)−Mo(1)−P(1)	171.04(5)	S(3)−Mo(1)−S(1)	120.92(5)
S(3)−Mo(1)−S(4)	109.19(5)	S(3)−Mo(2)−S(4)	107.33(5)
P(2)−Mo(2)−P(3)	166.79(5)		

$Mo_4S_6(SH)_2(PMe_3)_6$ (5H). In analogy to the preparation of **3H**, onto a frozen slurry of 300 mg (1.15 mmol) of $(NH_4)_2MoS_4$ in 10 mL of MeCN was condensed 0.7 mL (6.8 mmol) of PMe_3 and 310 mg (9.1 mmol) of H_2S. The vessel was evacuated, sealed, and then allowed to warm to room temperature. The slurry was stirred for 3 h during which it turned green and eventually a brown microcrystalline precipitate began to form. The flask was then left undisturbed for 2 h further during which the solution turned brown and brown microcrystals formed, which were isolated by removal of the solvent via cannula. Yield: 250 mg (80%). This material was invariably contaminated with $SPMe_3$, and the yield was estimated by ^{1}H NMR determination of the **5H**/$SPMe_3$ ratio. ^{1}H NMR (C_6D_6, 500 MHz, 298 K): δ 2.74 (d, 2H), 1.77 (d, 18H), 1.45 (m, 36). ^{31}P NMR (C_6D_6, 298 K): δ 2.24 (q, 2P), −23.98 (t, 4P). Alternatively, **5H** can be made from **3H** by simply allowing a MeCN solution of **3H** at room temperature to stand overnight. The solution turns brown, and brown microcrystals form. This process is greatly accelerated through the addition of excess H_2S (>10 equiv).

$Mo_4S_6(SEt)_2(PMe_3)_6$ (5Et). A solution of 10 mL of MeCN and 0.2 mL of EtSH (2.7 mmol) was added to 200 mg (0.43 mmol) of **2**. The mixture was stirred for 3 h with a brisk N_2 purge and then left undisturbed overnight during which the solution turned brown and brown microcrystals formed, which were isolated by removal

of the solvent via cannula. Yield: 198 mg (40%). This material was invariably contaminated with $SPMe_3$, and the yield was estimated by ^{1}H NMR determination of the **5Et**/$SPMe_3$ ratio. ^{1}H NMR (C_6D_6, 500 MHz, 298 K): δ 3.57 (q, 4H), 1.94 (d, 18H), 1.46 (t, 6H), 1.43 (m, 36H). ^{31}P NMR (C_6D_6, 298 K): δ −0.34 (q, 2P), −24.01 (t, 4P).

$W_4S_6(SH)_2(PMe_3)_6$. Onto a frozen slurry of 300 mg (0.84 mmol) of $(NH_4)_2WS_4$ in 10 mL of MeOH and 10 mL of MeCN was condensed 0.7 mL (6.8 mmol) of PMe_3 and 310 mg (9.1 mmol) of H_2S. The vessel was evacuated, sealed, and then allowed to warm to room temperature. Over the course of 12 h, the solution assumed a dark green coloration. This solution was placed in the freezer for 4 days to allow crystals to grow. The resulting green crystals were isolated by decanting the solution and drying in vacuo. Yield: 20 mg (9%). ^{1}H NMR (C_6D_6, 500 MHz, 298 K): δ 3.66 (d, 2H), 1.85 (d, 9H), 1.53 (m, 18H). ^{31}P NMR (C_6D_6, 298 K): δ −26.80 (m, 2P), −59.54 (t, 4P).

Crystallography. Crystals of $(NH_4)_2$**1**, **3Et**, **3H**, **3tol**, **4Et**, **5Et**, and **5H** were mounted on a thin glass fiber by using oil (paratone-N, Exxon) before being transferred to the diffractometer. Data were collected on a Siemens CCD automated diffractometer at 193 K. Data processing was performed with the integrated program package SHELXTL. All structures were solved using direct methods or Patterson maps and refined using full-matrix least-squares on SHELXTL V6 (Bruker, 2001). Methyl H atom positions for PMe_3 were optimized by rotation about P−C bonds with idealized C−H distances. S-*H* atoms were all located. H atom *U* values were assigned on the basis of the U_{eq} of adjacent non-H atoms. The data were corrected for absorption on the basis of face centered scans. Specific details for each crystal are given in Table 1, and bond lengths and angles for **3Et** are provided in Table 2. Full crystallographic data for **3Et**, **3H**, **3tol**, **4Et**, **5Et**, and **5H** have been deposited with the Cambridge Crystallographic Data Center as supplementary publication numbers 197576 (**3H**), 197577 (**4Et**), 197578 (**3Et**), 197579 (**3tol**), 197580 (**5Et**), and 197581 (**5H**).

Acknowledgment. This research was supported by the NSF. We thank Steve Smith for assistance with the synthesis of $MoS_2(dmpe)_2$.

Supporting Information Available: X-ray data for $(NH_4)_2$**1**, **3H**, **3Et**, **3tol**, **4Et**, **5H**, **and 5tol**and the ^{1}H{^{31}P} NMR spectra for **3H**. This material is available free of charge via the Internet at http://pubs.acs.org.

IC026215M